



# Intermolecular coupling and fluxional behavior of hydrogen in phase IV

HPSTAR  
863-2019

Alexander F. Goncharov<sup>a,b,1</sup>, Irina Chuvashova<sup>b</sup>, Cheng Ji<sup>c,1</sup>, and Ho-kwang Mao<sup>c,1</sup>

<sup>a</sup>Center for Energy Matter in Extreme Environments, Key Laboratory of Materials Physics, Institute of Solid State Physics, Chinese Academy of Sciences, 230031 Hefei, Anhui, China; <sup>b</sup>Geophysical Laboratory, Carnegie Institution of Washington, Washington, DC 20015; and <sup>c</sup>Center for High Pressure Science and Technology Advanced Research, 201203 Shanghai, China

Contributed by Ho-kwang Mao, October 25, 2019 (sent for review September 24, 2019; reviewed by Roberto Bini and Yanming Ma)

**We performed Raman and infrared (IR) spectroscopy measurements of hydrogen at 295 K up to 280 GPa at an IR synchrotron facility of the Shanghai Synchrotron Radiation Facility (SSRF). To reach the highest pressure, hydrogen was loaded into toroidal diamond anvils with 30- $\mu$ m central culet. The intermolecular coupling has been determined by concomitant measurements of the IR and Raman vibron modes. In phase IV, we find that the intermolecular coupling is much stronger in the graphenelike layer (G layer) of elongated molecules compared to the Br<sub>2</sub>-like layer (B layer) of shortened molecules and it increases with pressure much faster in the G layer compared to the B layer. These heterogeneous lattice dynamical properties are unique features of highly fluxional hydrogen phase IV.**

hydrogen | infrared spectroscopy | high pressure | diamond anvil cell

Dense hydrogen demonstrates a number of fascinating phenomena (1), and theory predicts even more spectacular behaviors at higher pressures, which remained to be explored (2, 3). Of particular interest is a behavior related to an increase of the kinetic energy and thus quantum atomic motion, which may lead to a change in the character of the chemical bonds (4) or even to a decline in the melting temperature, which can ultimately result in a liquid ground state (5, 6). Hydrogen with the lightest atoms manifests the most suitable system to explore such effects. However, reaching the appropriate states requires very high pressures, which remains technically challenging.

Static high-pressure techniques have been recently progressing aggressively stimulated by scientific goals of better understanding materials under extremes (e.g., in planetary interiors), competition with dynamic compression techniques, and new advances in first-principles calculations. High-pressure molecular hydrogen (H<sub>2</sub>) is expected to transform to a metallic monatomic state at high pressures (7, 8) [its synthesis is under debate (9)], but the route remained unclear. Until 2012, only 3 molecular phases of H<sub>2</sub> had been widely recognized: plastic (fully orientationally disordered) hexagonal close-packed (hcp) phase I and orientationally ordered phases II and III at low temperature and high pressure. While phase II, possessing quantum ordering features (10, 11), is unusual for molecular crystals, phase III was thought to be similar to common orientationally ordered phases in other classical molecular crystals such as diatomics (12). Assuming that this behavior continues to higher pressures, one could expect that higher-pressure H<sub>2</sub> polymorphs would be classically ordered molecular crystals as the density-functional theory (DFT) predicts (12). However, experiments revealed an unusual “mixed molecular and atomic” phase, named phase IV, to crystallize at 225 GPa on compression of phase I via phase III at 295 K (4, 6). The originally identified structural model, *Pbcn* (12), was found to be slightly less stable than *Cmca-4* in DFT calculations (12–14). Recent diffusion quantum Monte Carlo calculations showed that *Pc-48* is more stable at close to room temperatures (15) for phase IV. The model has two types of molecules, elongated molecules in graphenelike layers (G layers) and shortened molecules in quasihexagonal layers (B layers), to account for the 2

vibrons with distinct pressure responses (see *SI Appendix, Fig. S1* for the illustration of G layer and B layer).

However, all this classical structural picture has been questioned in molecular-dynamics simulations (16–19), showing that the structure of this phase is highly dynamic, where the atoms in the elongated molecules of G layers show a diffusive motion, which can be viewed as the rotation of a 3-molecule ring and an even longer atomic migration. Thus, the chemical bonds change their space location migrating with time yet preserving the local lattice symmetry at each time; we call this behavior fluxional in analogy with that of some molecular substances at ambient conditions (20). On the other hand, the shortened molecules in B layers are orientationally disordered but the atoms do not migrate between the molecular sites. Very recent X-ray diffraction (XRD) experiment indicates that phase IV has an hcp structure with higher symmetry than all theoretically predicted structures (21). Fluxional behavior may produce a time-average effect to increase the apparent symmetry.

Previous optical spectroscopy investigations (4, 22–24) demonstrated that phase IV has Raman and IR spectra, distinct from the phases discovered earlier, characterized by the presence of 2 vibron modes (in G layers and B layers); the lower-frequency vibron modes ( $\nu_1$ ) show a softening and broadening behavior under pressure which is consistent with the molecules in the G layers to be very short lived (16, 17). In contrast, the higher-frequency vibron ( $\nu_2$ )

## Significance

Transformations of solid hydrogen at very high pressures are of fundamental interest as this behavior provides a benchmark for other materials. Molecular hydrogen is expected to transform to a monatomic solid at very high pressures; however, intermediate states and their existence remain largely unexplored. Quantum atomic motion is expected to play an increased role for these highly compressed states. Here we revisit hydrogen phase IV, which was reported to exhibit mixed molecular-atomic configurations, to probe the intermolecular interaction in this intermediate regime. By employing concomitantly synchrotron infrared and conventional Raman spectroscopy on the same sample, we do find that the intermolecular interactions are greatly heterogeneous, providing unique experimental insights into vibrational dynamics and lattice fluxionality of hydrogen in phase IV.

Author contributions: A.F.G. and H.-k.M. designed research; A.F.G. and C.J. performed research; A.F.G. contributed new reagents/analytic tools; A.F.G. and I.C. analyzed data; and A.F.G., I.C., C.J., and H.-k.M. wrote the paper.

Reviewers: R.B., University of Florence and Y.M., Jilin University.

The authors declare no competing interest.

Published under the [PNAS license](#).

<sup>1</sup>To whom correspondence may be addressed. Email: agoncharov@carnegiescience.edu, cheng.ji@hpstar.ac.cn, or maohk@hpstar.ac.cn.

This article contains supporting information online at <https://www.pnas.org/lookup/suppl/doi:10.1073/pnas.1916385116/-DCSupplemental>.

First published December 3, 2019.

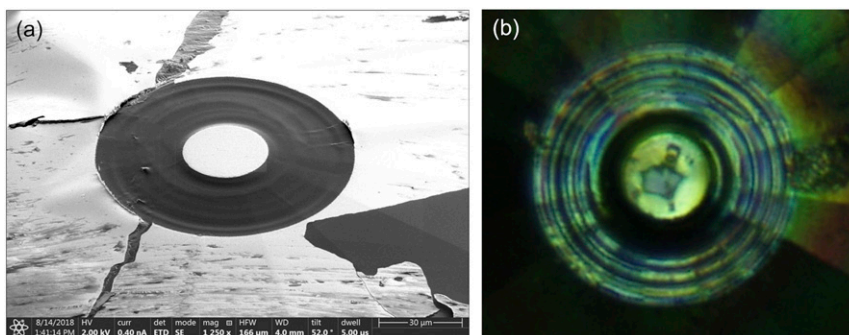


**Fig. 1.** Loading of hydrogen with the toroidal diamond anvils. (A) scanning electron microscope image of the diamond tip machined with FIB. (B) Optical microscope image of the loaded hydrogen sample in the transmitted and reflected light at  $\sim 160$  GPa.

corresponds to shortened molecules in B layers. However, Raman and IR experiments have been performed separately, making it difficult to compare the results, especially concerning the splitting between the IR and Raman modes. The difference between IR and Raman frequency of a vibron mode provides valuable information on the intermolecular coupling of the mode. Here, we report the results of concomitant IR/Raman experiments on the same sample yielding reliable information about the intermolecular coupling in both G- and B layers. We find that the intermolecular coupling in the 2 types of layers are very different, with that in the G layers being much stronger and increasing more rapidly with compression compared to that in B layers.

Two (out of a dozen attempts) diamond anvil cell experiments were successful in reaching pressures in excess of 200 GPa which are needed to reach phases III and IV of hydrogen at 295 K. One was performed to 240 GPa using conventional single-beveled diamonds with 40- $\mu\text{m}$  tip diameter. The other one used toroidal anvils (25, 26) machined with focused ion beam (FIB) from conventional beveled anvils with 50- $\mu\text{m}$  tip diameter, yielding 30- $\mu\text{m}$ -diameter tips (Fig. 1A). The use of the toroidal anvil configuration eventually targets at achieving higher pressures than using the conventional beveled anvils. These anvils were coated (using sputtering) with alumina of 50–100-nm thickness. Rhenium was used as the gasket. Hydrogen was loaded at room

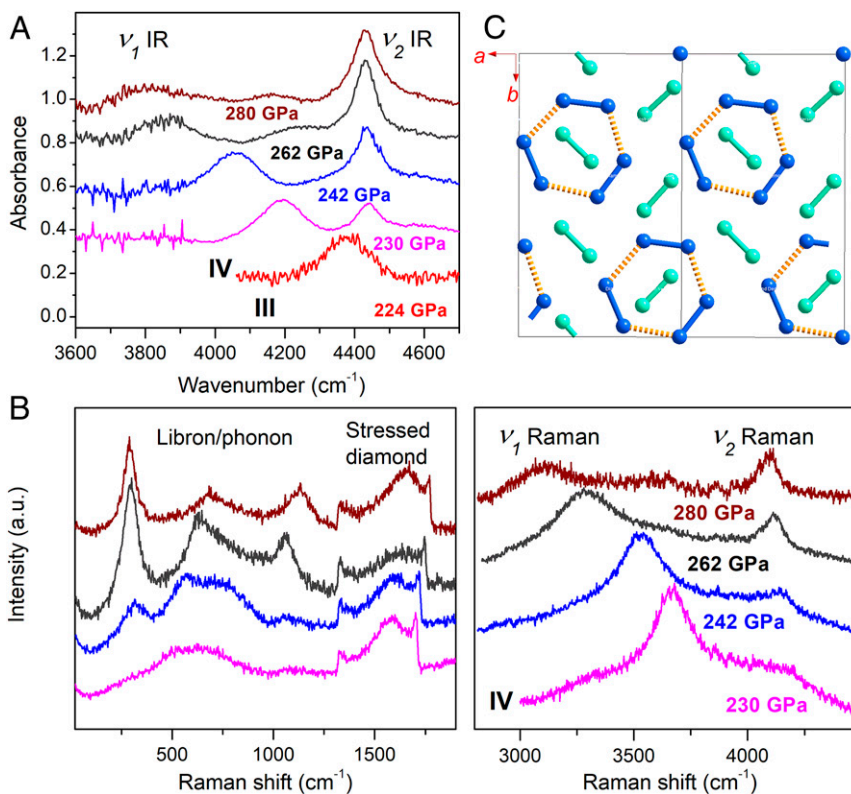


**Fig. 2.** Synchrotron IR and Raman spectroscopy in compressed hydrogen up to 280 GPa at 295 K. (A) IR spectra of the vibron modes in phases III and IV. (B) Raman spectra of phase IV as pressure increases; *Left* and *Right* show the libron plus phonon modes and the vibron modes, respectively. The vibron modes denoted as  $\nu_1$  and  $\nu_2$  correspond to the strongly and weakly bounded G and B layers, respectively. The results are in a qualitative agreement with previous measurements (4, 6, 22–24). (C) Configuration of G layers and B layers in the  $P_c$ -48 model (15). G layers contain the elongated molecules (blue intramolecular bonds) associated in quasi-hexagons (yellow intermolecular bond), while the B layers consist of shortened molecules (green bond). Only 2 layers are shown projected along the  $c$  axis.

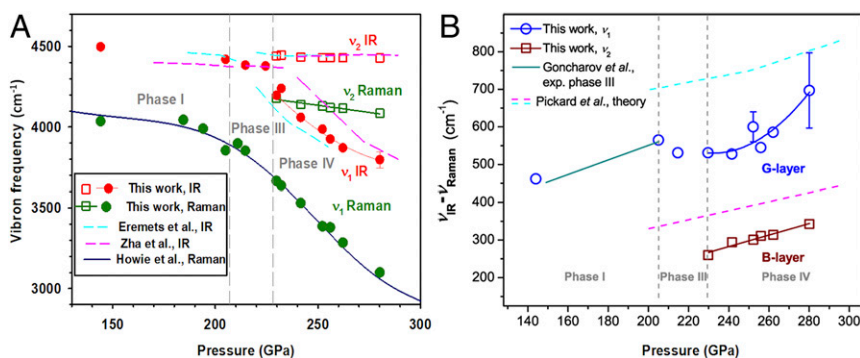


**Fig. 3.** (A) Raman and IR vibron frequencies as a function of pressure: symbols are from this work; pressure is determined via Raman measurements of the stressed anvils and further corrected to match the position of the main Raman vibron mode  $\nu_1$  according to the calibration of ref. 31. An uncertainty of the frequency determination is smaller than the size of the symbols except for the last pressure point, where an asymmetric  $\nu_1$  IR peak was observed; the IR results of ref. 23 agree fairly with Zha et al. (24) and are not shown. (B) Intermolecular coupling represented by the difference between the IR and Raman vibron frequencies: symbols are from this work and dashed lines are theoretically calculated (14); the results below 205 GPa are compared to previously measured in phase III (35).

temperature, being pumped up to 150 MPa using a compressor. The sample dimensions were  $\sim 10$   $\mu\text{m}$  at 160 GPa, as shown in Fig. 1B, and 6  $\mu\text{m}$  at the highest pressure of 280 GPa.

The IR spectra of the vibron modes (Fig. 2A) show an increase in intensity at the transition to phase III, where 1 strong vibron mode is observed (27). Above 224 GPa, this mode abruptly splits giving rise to a doublet (Fig. 2A). The lower-frequency  $\nu_1$ , corresponding to the G-layer molecules, softens and broadens with pressure, while the higher-frequency  $\nu_2$ , corresponding to B-layer molecules, is almost pressure independent and is gaining the intensity. The distinct pressure responses of the two bands indicate the existence of 2 types of molecules in phase IV. Concomitant Raman measurements at the same conditions (Fig. 2B) show a similar behavior of the Raman vibron band albeit the frequencies are shifted to lower energies. This energy distinction is because Raman and IR vibron modes have different vibration patterns for the molecules that belong to the same unit cell: in-phase for Raman and out-of-phase for IR active modes. Thus, the Raman-IR splitting value represents the strength of the intermolecular coupling (28, 29). The intermolecular coupling is commonly represented as Van Kranendonk's hopping matrix elements  $\varepsilon_{ij}$  (30), that correspond to intermolecular coupling strengths. For instance, the difference in the Raman and IR vibron frequency in hcp phase I of hydrogen is  $6\varepsilon$ , where  $\varepsilon/2$  corresponds to the pair interactions between nearest-neighbor molecules. Under pressure, the intermolecular coupling normally increases, representing a normal tendency for compression of molecular crystals, where intermolecular distances contract much faster than intramolecular (these can even expand) due to heterogeneity of the interatomic interactions. This behavior has been established for phases I, II, and III of hydrogen, but phase IV reveals an anomalous behavior as elaborated below.

Our combined concomitant IR-Raman experiments allow determining the splitting of the vibrational band independently of the pressure measurements. This is critical to accurately characterize the splitting, since such determination has been performed based on separate IR and Raman measurements, in which pressure determination could suffer a large uncertainty (e.g., ref. 31). Here, based on our improved measurements, we find a sharp increase of the intermolecular coupling strength with pressure in molecules belonging to G layers (Fig. 3B) especially in phase IV. The intermolecular coupling between molecules in B layers is obviously weaker. This 2-type-molecule scenario develops in phase IV with the G-layer molecules becoming fluxional. At these conditions ( $\geq 270$  GPa), the whole inter-/intramolecular bonding concept is about to break down in the G layer because the difference between

intra- and intermolecular bond strength becomes much less substantial. Moreover, the molecules in G layers are short living as they decompose and recombine within a picosecond timescale (16, 17); this dramatically increases anharmonic effects. On the other hand, the intermolecular coupling in B layers is much weaker, demonstrating an intriguing bonding distinction between molecules in G- and B layers, which also results in a charge transfer and band-gap opening (17) stabilizing the structure. Concerning the intermolecular bonding anisotropy, it can be explained naively as due to a difference in the intramolecular bond lengths in G- and B layers which leaves a complementary length for the intermolecular bonds in these adjacent layers. Thus, phase IV of hydrogen manifests a Peierls distortion of some kind.

Recently, technical breakthroughs have been made and XRD data of hydrogen at above 2-Mbar pressures became available, and disclosed the crystal structure of phase IV (21). Based on XRD results, the phase transitions along the 295 K isotherm, from phase I to phases III and IV, appear to be isostructural. XRD probes the scattering from electrons which are located in between 2 hydrogen atoms in 1 molecule, thus captures an average over the time positions of the mass centers of  $\text{H}_2$  molecules. Noteworthy, vibrational spectroscopy is complementary to XRD since the former is sensitive to the local symmetry of molecules. Even though the XRD results suggest the mass center of  $\text{H}_2$  molecules sit on hcp-like lattice in phase IV, Raman and IR data clearly indicate the emerging of 2 types of distinct  $\text{H}_2$  molecules, while XRD is insensitive to such symmetry breaking at the molecular level. By considering both XRD and spectroscopy data, when the hcp Brillouin zone gets highly distorted under strong compression (21), hydrogen appears to develop 2 types of molecules, in phase IV, with one being strongly interacting with neighbors and fluxional in G layers and the other with weaker intermolecular coupling in B layers. Since the molecules in G layers are fluxional, the time-averaged symmetry in both of the layers is still hexagonal, thus consistent with the XRD measurements (SI Appendix, Fig. S3). With further compression, the intensified intermolecular interactions between the G-layer molecules may eventually lead to equal intermolecular and intramolecular distances, viz., the breakdown of the molecular configuration. At 280 GPa, our experiment demonstrates that the band gap is still open in phase IV (Fig. 4), in agreement with previous observations (4). Vibrational spectroscopy represents a unique way of probing this unusual high-pressure behavior capturing a local atomic configuration to which it is very sensitive.

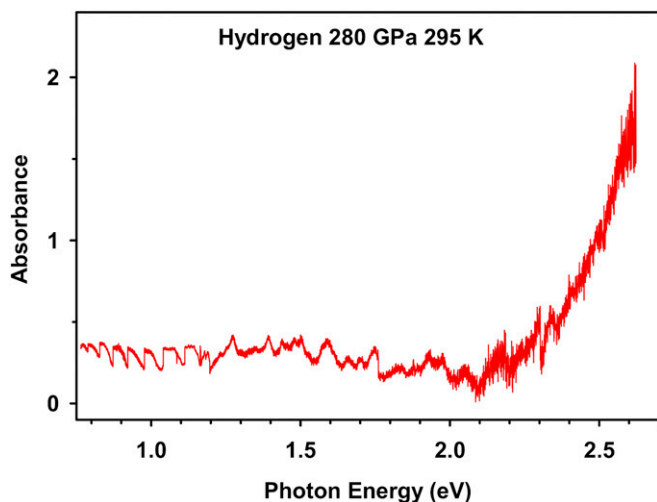


Fig. 4. Optical absorption spectrum of hydrogen at 280 GPa obtained concomitantly with IR and Raman spectroscopy measurements of Fig. 2.

## Methods

We performed the experiments at a newly constructed system at the beamline BL01B of the Shanghai Synchrotron Radiation Facility (32, 33). The system combines synchrotron Fourier-transform (FTIR) spectroscopy with a broadband laser visible/IR and conventional laser Raman spectroscopy in one instrument. The all-mirror custom confocal IR microscope was used in a transmission mode and the FTIR spectra were recorded with a mercury-cadmium-telluride

detector with the  $0.05 \times 0.05\text{-mm}^2$  crystal dimensions in the spectral range of  $700\text{--}10000\text{ cm}^{-1}$ . The synchrotron beam diameter was about  $10\text{ }\mu\text{m}$  measured in the IR spectral range (33). The transmission IR measurements were performed in a single-channel mode using the IR spectrum of the same sample measured at the condition where IR absorption was relatively weak (e.g., in phase I) (28) as the reference. The same IR optics was used to measure visible and IR transmission spectra with the Raman spectrometer equipped with array charge-coupled device (CCD) and IR detectors. The Raman microscope objective lens (Mitutoyo 50 $\times$ , N.A. = 0.4) is interchangeable with the IR reflective objectives diverting the optical path to the Raman spectrometer. A 660-nm single-line solid-state laser was used to excite the Raman spectra in a backscattering geometry and the signal was analyzed using 3 narrow bandpass notch filters and a single-grating 500-mm-focal-length spectrograph equipped with a CCD detector. Raman and IR experiments were performed at 295 K at the same nominal pressure measured with Raman spectra of the stressed diamond (34) and finely corrected using the spectral position of the main Raman vibron band as presented in ref. 31.

**Data Availability.** The data that support the findings of this study are included in *SI Appendix*.

**ACKNOWLEDGMENTS.** We thank S. Vitale and Z. Geballe for FIB machining of the diamond anvils and Lingping Kong for help with the IR synchrotron beamline. This work was supported by the National Natural Science Foundation of China (Grants 51672279, 51727806, 11874361, 11774354, and U1930401), Science Challenge Project (Grant TZ2016001), and the CASHIPS Director's Fund (Grant YZJJ201705), the NSF EAR-1763287, the Army Research Office, the Deep Carbon Observatory, and the Carnegie Institution of Washington. A.F.G. was partially supported by the Chinese Academy of Sciences Visiting Professorship for Senior International Scientists (2011T2J20) and the Recruitment Program of Foreign Experts.

- J. M. McMahon, M. A. Morales, C. Pierleoni, D. M. Ceperley, The properties of hydrogen and helium under extreme conditions. *Rev. Mod. Phys.* **84**, 1607–1653 (2012).
- E. Babaev, A. Sudbø, N. W. Ashcroft, A superconductor to superfluid phase transition in liquid metallic hydrogen. *Nature* **431**, 666–668 (2004).
- E. Babaev, A. Sudbø, N. W. Ashcroft, Observability of a projected new state of matter: A metallic superfluid. *Phys. Rev. Lett.* **95**, 105301 (2005).
- R. T. Howie, C. L. Guillaume, T. Scheler, A. F. Goncharov, E. Gregoryanz, Mixed molecular and atomic phase of dense hydrogen. *Phys. Rev. Lett.* **108**, 125501 (2012).
- S. A. Bonev, E. Schwegler, T. Ogitsu, G. Galli, A quantum fluid of metallic hydrogen suggested by first-principles calculations. *Nature* **431**, 669–672 (2004).
- M. I. Eremets, I. A. Troyan, Conductive dense hydrogen. *Nat. Mater.* **10**, 927–931 (2011).
- E. Wigner, H. B. Huntington, On the possibility of a metallic modification of hydrogen. *J. Chem. Phys.* **3**, 764–770 (1935).
- E. G. Brovman, Y. Kagan, A. Kholas, Properties of metallic hydrogen under pressure. *J. Exp. Theor. Phys.* **35**, 783 (1972).
- H. Y. Geng, Public debate on metallic hydrogen to boost high pressure research. *Matter Radiat. Extremes* **2**, 275–277 (2017).
- I. I. Mazin, R. J. Hemley, A. F. Goncharov, M. Hanfland, H.-k. Mao, Quantum and classical orientational ordering in solid hydrogen. *Phys. Rev. Lett.* **78**, 1066–1069 (1997).
- G. Geneste, M. Torrent, F. Bottin, P. Loubeyre, Strong isotope effect in phase II of dense solid hydrogen and deuterium. *Phys. Rev. Lett.* **109**, 155303 (2012).
- C. J. Pickard, R. J. Needs, Structure of phase III of solid hydrogen. *Nat. Phys.* **3**, 473–476 (2007).
- H. Liu, L. Zhu, W. Cui, Y. Ma, Room-temperature structures of solid hydrogen at high pressures. *J. Chem. Phys.* **137**, 074501 (2012).
- C. J. Pickard, M. Martinez-Canales, R. J. Needs, Density functional theory study of phase IV of solid hydrogen. *Phys. Rev. B* **85**, 214114 (2012).
- N. D. Drummond *et al.*, Quantum Monte Carlo study of the phase diagram of solid molecular hydrogen at extreme pressures. *Nat. Commun.* **6**, 7794 (2015).
- H. Liu, Y. Ma, Proton or deuteron transfer in phase IV of solid hydrogen and deuterium. *Phys. Rev. Lett.* **110**, 025903 (2013).
- A. F. Goncharov *et al.*, Bonding, structures, and band gap closure of hydrogen at high pressures. *Phys. Rev. B* **87**, 024101 (2013).
- H. Liu, J. Tse, Y. Ma, Robust diffusive proton motions in phase IV of solid hydrogen. *J. Phys. Chem. C* **118**, 11902–11905 (2014).
- I. B. Magdãu, G. J. Ackland, Identification of high-pressure phases III and IV in hydrogen: Simulating Raman spectra using molecular dynamics. *Phys. Rev. B* **87**, 174110 (2013).
- F. A. Cotton, Fluxional organometallic molecules. *Acc. Chem. Res.* **1**, 257–265 (1968).
- C. Ji *et al.*, Ultrahigh-pressure isostructural electronic transitions in hydrogen. *Nature* **573**, 558–562 (2019).
- M. I. Eremets, I. A. Troyan, P. Lerch, A. Drozdov, Infrared study of hydrogen up to 310 GPa at room temperature. *High Press. Res.* **33**, 377–380 (2013).
- P. Loubeyre, F. Occelli, P. Dumas, Hydrogen phase IV revisited via synchrotron infrared measurements in H<sub>2</sub> and D<sub>2</sub> up to 290 GPa at 296 K. *Phys. Rev. B* **87**, 134101 (2013).
- C. S. Zha, Z. Liu, M. Ahart, R. Boehler, R. J. Hemley, High-pressure measurements of hydrogen phase IV using synchrotron infrared spectroscopy. *Phys. Rev. Lett.* **110**, 217402 (2013).
- A. Dewaele, P. Loubeyre, F. Occelli, O. Marie, M. Mezouar, Toroidal diamond anvil cell for detailed measurements under extreme static pressures. *Nat. Commun.* **9**, 2913 (2018).
- Z. Jenei *et al.*, Single crystal toroidal diamond anvils for high pressure experiments beyond 5 megabar. *Nat. Commun.* **9**, 3563 (2018).
- M. Hanfland, R. J. Hemley, H.-k. Mao, Novel infrared vibron absorption in solid hydrogen at megabar pressures. *Phys. Rev. Lett.* **70**, 3760–3763 (1993).
- M. Hanfland, R. J. Hemley, H.-k. Mao, G. P. Williams, Synchrotron infrared spectroscopy at megabar pressures: Vibrational dynamics of hydrogen to 180 GPa. *Phys. Rev. Lett.* **69**, 1129–1132 (1992).
- L. Cui, N. H. Chen, I. F. Silvera, Excitations, order parameters, and phase diagram of solid deuterium at megabar pressures. *Phys. Rev. B* **51**, 14987–14997 (1995).
- J. V. Kranendonk, *Solid Hydrogen* (Plenum, New York, 1983).
- R. T. Howie, E. Gregoryanz, A. F. Goncharov, Hydrogen (deuterium) vibron frequency as a pressure comparison gauge at multi-Mbar pressures. *J. Appl. Phys.* **114**, 073505 (2013).
- X. Zhou *et al.*, The BL01B1 infrared beamline at Shanghai synchrotron radiation facility. *Infrared Phys. Technol.* **94**, 250–254 (2018).
- A. F. Goncharov, L. Kong, H.-k. Mao, High-pressure integrated synchrotron infrared spectroscopy system at the Shanghai Synchrotron Radiation Facility. *Rev. Sci. Instrum.* **90**, 093905 (2019).
- Y. Akahama, H. Kawamura, Pressure calibration of diamond anvil Raman gauge to 310 GPa. *J. Appl. Phys.* **100**, 043516 (2006).
- A. F. Goncharov, R. J. Hemley, H.-k. Mao, J. Shu, New high-pressure excitations in parahydrogen. *Phys. Rev. Lett.* **80**, 101–104 (1998).